Uncertainty in flood discharges from urban and small rural catchments due to inaccurate head measurement

A. Petersen-Øverleir[1] and T. Reitan[2]

Hydrological Department, Norwegian Water Resources and Energy Directorate, PO Box 5091, Majorstua, N-0301 Oslo, Norway. E-mail: *apoe@nve.no*

Division of Statistics and Insurance Mathematics, Department of Mathematics, University of Oslo, PO Box 1053, Blindern, 0316 Oslo, Norway

Received 7 June 2004; accepted in revised form 20 September 2004

Abstract Despite frequent use of estimated flood discharges from urban and small rural catchments, the assessment of uncertainty in instantaneous discharge due to inaccurate head measurements is generally not performed. The present work discusses the impact of inaccurate head measurement on observed instantaneous flood discharge. The sources and sizes of uncertainties in head determination are discussed. A simple uncertainty model is developed in order to quantify the uncertainty in error-corrupted instantaneous and mean discharge. It is shown that uncertainty in mean discharge is less affected by uncorrelated head measurement error, while instantaneous discharges are substantially affected. Practical modelling using data from a Norwegian urban gauging station is undertaken. It is shown that the estimated annual maximum instantaneous flood discharge from this watershed has 95% confidence limits with sizes of 17–19% of the estimated discharge for average head measurement accuracy. Furthermore, it is shown that variability in head determination causes only a minor potential for bias in estimated instantaneous flood population statistics and quantiles.

Keywords Flood frequency analysis; head measurement; hydrometry; instantaneous discharge; uncertainty

Nordic Hydrology **Vol 36 No 3 pp 245–257** © IWA Publishing 2005

Introduction

Sustainable control over contamination and ecological impairment due to flooding is important in the assessment of residential watersheds (Novotny *et al.* 2001; Blake *et al.* 2003). Furthermore, flood control in order to reduce the impact of stormwater in urban drainage systems is essential in the design and operation of urban catchments (Marsalek *et al.* 1993).

Considering potential flooding from small rural catchments is important in areas such as road-culvert design (La Marche and Lettenmaier 2000) and contamination, erosion and sediment transport analysis for small cultivated watersheds (Andersen *et al.* 1999; Beuselinck *et al.* 2000; Cerdan *et al.* 2002).

The availability of high quality streamflow data is important in order to perform the above types of flood analyses. Urban and small rural catchments floods are characterised by rapid flood generation. Flood build-up, culmination and recession can happen within minutes (see Fig. 3), making high time resolution an essential feature in data collection and flood frequency analysis for these types of catchments. Traditional discharge measurements using current meter, dilution, etc., are generally unavailable since; 1) the water level changes very fast during floods and 2) they are often unusable due to very small discharges. This makes it almost impossible to build up a rating curve from discharge measurements. Weirs and flumes with theoretical head–discharge equations are often applied in these types of situations in order to obtain streamflow data. Such installations, if selected, constructed and maintained

properly, can give rise to surprisingly accurate head–discharge relationships with an attainable accuracy of 1% (Herschy 1999b). However, such accuracy is extremely dependent on how exactly the head is measured.

An estimated discharge is not complete without presenting its uncertainty. However, uncertainty in streamflow data due to hydrometric errors is generally overlooked in hydrological flood frequency analysis, although some exceptions exists (Potter and Walker 1981; Rosso 1985; Kuczera 1992; Clarke 1999).

Uncertainty in large instantaneous discharge estimates due to inaccurate head measurement is almost negligible compared to other sources of uncertainty, such as rating curve variability. However, incorrect head measurement becomes noticeable for small instantaneous discharges.

In the present work we assume the head–discharge equation to be absolutely correct in order to exclusively analyse the effect inaccurate head measurement has on estimated instantaneous flood discharges from small and flashy catchments. The first section discusses the sources, sizes and statistical distribution of the uncertainty in head determination. The next section presents the discharge uncertainty model which is then applied to actual flood data from a small urban catchment in Norway in the following section. The final section shows theoretically how inaccurate head determination causes little bias in estimated flood quantiles and a negligible potential misspecification of flood population statistics.

Head measurement

Sources of repeating uncertainty

Once the appropriate location for head measurement is found, the method of measurement must be selected. The most common technique in many countries, including Nordic countries, is the float gauge. The float is usually placed in a stilling well connected to the approach channel by an inlet pipe, while sometimes the float is placed directly in the approach channel. Modern floats are usually connected to a rotating optical encoder wheel by a beaded wire with a counterweight. The encoder is further electrically connected to a recorder which transforms the digital signals caused by rotation from the wheel into head. The head measurement accuracy that is possible using an encoder is primarily determined by; 1) the resolution of the optical encoder (typically, ± 2–5 mm); and 2) the electrical and mechanical encoder performance. The manufacturers often give the accuracy of the actual encoder in $\pm$ mm. This uncertainty is often interpreted as uniformly distributed by technicians. However, it is unclear whether this interpretation is correct, or whether the numbers given are the standard deviation calculated from laboratory testing. This study interprets the encoder uncertainty as normally distributed. Additional uncertainties involved with float measurement may be; 1) partly clogged inlet pipe; 2) friction between the float and the stilling well; 3) the beaded wire spins on the optical encoder wheel; 4) change in mass of float caused by algae growth and hard matter deposition; 5) drag forces and position of the float different from that obtained during calibration; 6) variable float buoyancy due to changeable equilibrium between the float and the counterweight; and 7) waves and ripples on the water surface. This study considers the total uncertainty involved with float measurements as normally distributed.

Another commonly used technique is to determine the head by a pressure transducer, which transforms the variation in water level into analogue changing electrical signals which are further logged on the recorder. The accuracy of a pressure transducer is usually presented as the percentage of the range in the water level which the pressure transducer is meant to cover, for example 0.25% of a range of 0–1 m, which usually is considered as a uniformly distributed uncertainty of ± 2.5 mm. This uncertainty is often based on the limitations of the electrical components inside the transducer which operates with an accuracy that is

dependent on temperature. Additional uncertainties involved in pressure transducer measurement may be: 1) change in characteristics due to corrosion, settlement and deposition of sediments, 2) variation in water density, 3) inaccurate determination of atmospheric pressure and 4) surface waves and ripples. Although the basic uncertainty of the transducer typically is looked upon as uniformly distributed, the present study assumes the total uncertainty involved with the transducer is normally distributed.

Other methods not common in Scandinavia, such as gas purge gauges and ultrasonic gauges, are sometimes applied for stage measurements. These techniques will not be discussed in this paper. Nevertheless, the uncertainties involved in these methods have the same sizes as the float and pressure transducers (personal communication with Ott Instruments, Germany).

The measurement of water level must be frequently calibrated according to a reference gauge, of which the head is the distance between the crest of the control and the water surface. A vertical staff gauge placed in the stilling well or the approach channel is often used as the reference gauge. The resolution of the staff and the method for reading off the water level obviously dictates the accuracy of the calibration. Typical resolution for a gauging staff is 10 mm. However, additional use of finer equipment such as a high resolution ruler can improve calibration accuracy. Hence, we do not consider calibration uncertainty in the present study, and assume that the variability of the staff reading is negligible. Another reason for doing this is due to statistical tractability. Variability in calibration is not a repeating random variable. Consequently, including it would have distorted most of the subsequent analysis, in much the same way as including uncertainty in the head–discharge relationship into the analysis.

It is difficult to give single universal figures for the total accuracies of the head gauging methods described. However, Ackers *et al.* (1978) present the uncertainty of a float in a stilling well as ± 6 mm. The text does not reveal whether this number is the standard deviation. Keeland *et al.* (1997) report standard deviations in the range 1.4–40 mm involved with pressure transducers. From our experience at NVE (Norwegian Water Resources and Energy Directorate) standard deviations are generally about 4–20 mm.

Another type of repeating uncertainty, particular for head measurement during flood culmination, is connected with the time resolution of the recording. A flood peak is parabolic in shape and the recorded value will only coincidentally be at the top of the parabola. Figure 3 illustrates this as the flood peak is cut between two recorded values. Consequently, it is uncertain how high the correct culmination head is, and the size of this uncertainty is clearly proportional to the time resolution. However, this type of uncertainty will be negligible if time resolution is fairly high, as shown in Fig. 3 where the error magnitude is about 1–2 l/s. Thus, we do not include this type of uncertainty in this study. However, if the time resolution is not satisfactory, this cutoff error can be noticeable. Furthermore, it is not easy to handle statistically. First, the observed head will be affected by both bias (underestimation) and variability due to the cutoff. Also, the magnitude of both bias and variability due to cutoff will depend on the steepness of the hydrograph before and after the flood culmination. This type of dependence is not easy to quantify, making error modelling including cutoff effects difficult.

A simple head measurement error model

The previous section illustrated some of the assumed normally distributed uncertainties involved with water level measurement which make it impossible to determine the absolute true head. If we also assume to measure the true head (no bias), the following model can be presented:

$$\hat{w} = w + \varepsilon, \quad \varepsilon \sim N(0, \sigma^2) \tag{1}$$

where w is the true head, $\hat{w}$ is the observed head and σ is the standard deviation of the head measurement error.

In this paper we define three types of accuracies, based on experiences done at NVE, which are able to record the head in 95% of the cases within ±4 mm of the true head (high accuracy), within ±8 mm of the true head (medium accuracy) and within ±15 mm of the true head (low accuracy). This means

- $\sigma = 0.0020$ m ⟶ high accuracy
- $\sigma = 0.0040$ m ⟶ medium accuracy
- $\sigma = 0.0075$ m ⟶ low accuracy.

It is worth noting that these figures are in accordance with recommended head measurement accuracy given in WMO (1994).

Uncertainty in estimated discharge due to inaccurate head measurement

The observed discharge for most weirs and flumes can be obtained from the head–discharge equation (Herschy 1999a)

$$\hat{q} = a\hat{w}^b \tag{2}$$

where $\hat{q}$ is the observed discharge, $\hat{w}$ is the observed head and a and b are parameters related to the geometry and the coefficient of discharge of the construction. More complicated discharge equations are sometimes applied in order to obtain laboratory accuracy, but these equations are not considered in the present work. Equation (2) assumes no velocity head.

$\hat{q}$ is the estimate of the true discharge $q = aw^b$ and we wish a 95% confidence interval with left- and right-tail limits denoted as $(\Delta_{0.025}, \Delta_{0.975})$, which are the 0.025 and the 0.975 quantiles of $\hat{q} - q$.

Using Eqs. (1) and (2) we obtain

$$\Delta = \hat{q} - q = a\hat{w}^b - a(\hat{w} + \varepsilon)^b. \tag{3}$$

Furthermore, using the results in Appendix A and replacing true head with observed head, which is the standard frequentist inferential methodology, gives the following accurate approximation of the distribution of Δ:

$$\Delta \sim \mathrm{N}(0, [a\hat{w}^{b-1}b\sigma]^2). \tag{4}$$

Hence, we obtain the 95% confidence limits for the estimated discharge as

$$\hat{q}_{95} = (\hat{q} - 1.96ab\sigma\hat{w}^{b-1}, \hat{q} + 1.96ab\sigma\hat{w}^{b-1}). \tag{5}$$

We also define the uncertainty ratio R as the span of the 95% confidence limit divided by the estimated discharge, formally written as

$$R = \frac{\hat{q}_{95}}{\hat{q}} \cdot 100\% = \frac{3.92b\sigma}{\hat{w}} \cdot 100\%. \tag{6}$$

Equation (6) can be interpreted as the relative uncertainty in the estimated instantaneous discharge.

Denoting the recording time resolution in minutes as N, the mean discharge value over kN minutes is estimated by

$$\bar{\hat{q}} = \frac{1}{k}\sum_{i=1}^{k} a\hat{w}_i^b. \tag{7}$$

A 95% confidence limits for a mean discharge, when only uncertainty in head measurement

is taken into account as a source of variability, is from Eq. (5) given by

$$\hat{\bar{q}}_{95} = \left(\hat{\bar{q}} - 1.96 \frac{ab\sigma}{k} \sqrt{\sum_{i=1}^{k} \hat{w}_i^{2(b-1)}},\ \hat{\bar{q}} + 1.96 \frac{ab\sigma}{k} \sqrt{\sum_{i=1}^{k} \hat{w}_i^{2(b-1)}} \right). \quad (8)$$

It is apparent that the confidence limits in Eq. (8) become negligible for typical mean discharge values such as the daily mean and the annual mean since the time resolution of modern recording usually is high. However, Eq. (8) is based on the assumption that $\mathrm{cov}(\varepsilon_i,\varepsilon_{i+1}) = 0$. If this assumption is incorrect, the consideration of consecutive error outcomes becomes more complex. As an example; gradual algae growth on the float will introduce autocorrelation into the uncertainty model. In this situation, we will have fewer independent errors than the assumed k, and consequently Eq. (8) will underestimate the variability of the mean discharge. This discussion is not continued here, as the present study focuses on instantaneous flood discharges.

Appendix A shows that the assumption that Eq. (4) should be sufficiently accurate in most cases. However, if the head considered is so low that this simplification lacks justification, the exact distribution of Φ given in Appendix A or Monte Carlo simulations can be applied in order to obtain the quantiles of Δ. Monte Carlo methods are also suitable for analysing the impact of head measurement uncertainty in more complicated head–discharge equations than Eq. (2).

Equation (6) illustrates that the exponent in the discharge equation, in addition to the head uncertainty described by σ, determines how significant the uncertainty is in instantaneous discharge. Furthermore, we see that the relative uncertainty becomes less influential as the head increases. However, in practical situations, the constant a also has to be considered in order to evaluate preferable head measurement accuracy and choice of weir. Figure 1 gives an example of Eq. (6) for two types of thin plate notch weirs and two thin plate v-notch weirs. The head–discharge equation used was $q = 1.74Lw^{1.5}$ (m^3/s) for the notches with crest length L and $q = (8/15)\sqrt{2g}C_d \tan(\mathrm{angle}/2)w^{2.5}$ (m^3/s) for the v-notches (C_d set to 0.578).

We see that the notch with crest length L equal to 0.6 m. has a larger uncertainty than: 1) the 120° v-notch for discharges up to around 45 l/s and 2) the 90° v-notch for discharges up to around 100 l/s. If the crest length lessens to 0.3 m the notch has better relative accuracy than: 1) the 120° v-notch for all discharges smaller than 300 l/s and 2) the 90° v-notch for discharges above around 18 l/s. We also see that the relative uncertainty becomes negligible for all notches as the discharge exceeds 300 l/s. However, at 300 l/s the head is: 1) 0.70.·.m

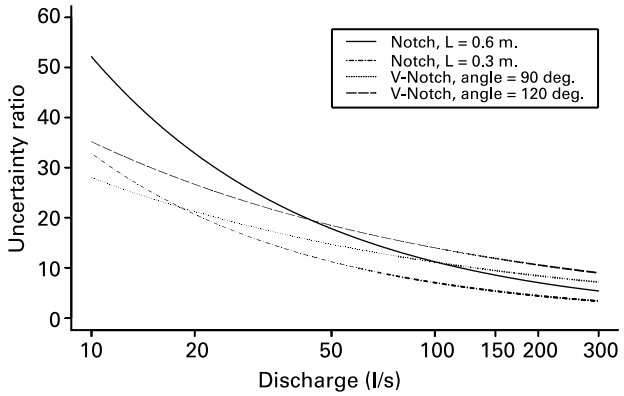

Figure 1 Uncertainty ratio plots for two thin plate notch weirs (crest lengths 0.3 and 0.6 m) and two thin plate v-notch weirs (angles 90° and 120°)

for notch L = 0.3, 2) 0.44 m for notch L = 0.6, 3) 0.55 m for v-notch 90° or 4) 0.43 m for v-notch 120°, which are figures that need consideration if available gauging height is an issue when designing the station.

Figure 2 is another example of the relative uncertainty in instantaneous discharge from a 90° thin plate v-notch weir. The plot illustrates the immense impact inaccurate head measurement has on the variability of the estimated instantaneous discharge. Head measurement of low accuracy causes a relative uncertainty greater than 15% in instantaneous discharges up to 200 l/s, while highly accurate head determination causes a lesser, but noticeable, relative instantaneous discharge uncertainty of down to 5% at 200 l/s. Nevertheless, the magnitudes of the uncertainties are of such a size that they should be considered in subsequent analyses.

A practical study

We will further analyse the impact of inaccurate head measurement by applying the results in the previous section to streamflow data from an urban watershed in Norway. The main features of the Sandsli gauging station are presented in Table 1. Sandsli is located near the city of Bergen on the west coast of Norway and records, in addition to rainfall, temperature and snow melting, discharge using a 134° thin plate v-notch weir. The maximum head capacity of the weir is 242 mm. This level has been exceeded once when an extremely intensive flood occurred in 2002.

The gauging station, which has excellent operational facilities such as heating and lighting, has collected discharge data of adequate quality since 1997. Streamflow from the urbanised catchment upstream is conveyed into an underground approach channel by a pipeline, where it runs over the weir and continues into a downstream culvert. Head is measured in a small stilling well next to the approach channel. A float connected to an optical encoder wheel by a steel wire measures the head. Flood generation occurs quickly at Sandsli. Figure 3 illustrates a summer flood in 2003, where heavy rainfall generated a flood which peaked 25 min after the first tip was detected on the rain gauge.

The accuracy in head measurement at Sandsli is considered to be medium according to the values presented in the first section, which implies a standard deviation of about 0.0040. The station is visited approximately once a month and the head read off the vertical gauging staff is compared to the recorded value. Figure 4 is a histogram of the differences between these values over the period 2000–2003. It is believed that the difference reflects the uncertainty in

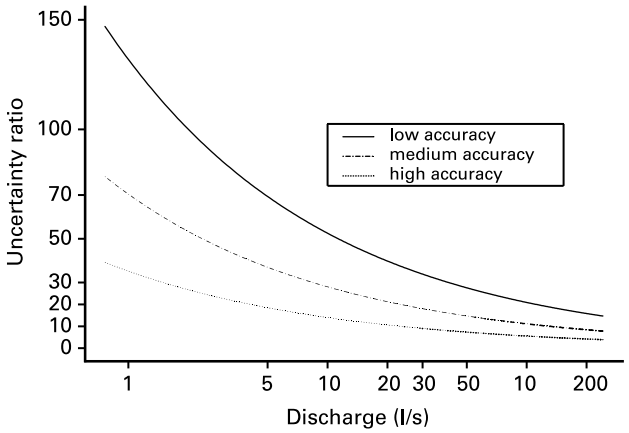

Figure 2 Uncertainty ratio plots for a thin plate v-notch weir with angle 90° for different sizes of head measurement accuracy

Table 1 Information about Sandsli gauging station

Name	Area	Area of impermable surfaces	Record	Time resolution	Head–discharge equation
56.1.0 Sandsli	0.080 km^2	0.014 km	1997–2003	1 min	$Q = 3.2764w^{2.5}$

head measurements since we assume that the gauging staff reading is correct. The empirical standard deviation of the differences is 3.57 mm, which is close to the assumed number. A Kolmogorov–Smirnov test was applied to the differences in order to test for normality and indicated no reason for rejecting a hypothesis of normal distributed differences.

Applying $\sigma = 0.0040$ into Eqs. (5) and (6) gives us the head–discharge relationship with 95% confidence limits and the relative uncertainty in estimated discharge at Sandsli. Figure 5 illustrates that the uncertainty of the rating curve due to inaccurate head measurement is quite noticeable. Furthermore, the relative instantaneous discharge uncertainty is especially large in the area of low to mean flow. The 95% confidence limits in Fig. 3 illustrate this effectively, as all the post-recession discharges have a relative uncertainty of 50%.

Seven years of data makes it impossible to perform a flood frequency analysis at Sandsli. Nevertheless, Table 2 illustrates the large variability of the annual maximum flood discharges due to uncertainty in head measurement. This kind of uncertainty in data is normally not considered in flood frequency inference.

Impact of inaccurate head measurement on instantaneous flood frequency analysis

The previous section illustrated that the annual maximum instantaneous discharge from a small watershed is significantly affected by uncertainty in head determination. It is often necessary to estimate the magnitude of a flood in a probabilistic sense since, from a frequentist perspective, hydrologic systems are driven by random input. Estimating the T-year flood instantaneous discharge typically involves fitting the observed annual maximum discharge, here denoted as X, to a probability model which often is based on one of the famous Fisher and Tippett (1929) extreme value distributions.

In real-life hydrology we observe only annual maximum instantaneous discharges more or less affected by variability in head determination, here denoted as Y, while it is the characteristics of the true annual maximum instantaneous discharges X which we are interested in. It is easily seen from Eq. (A9) that

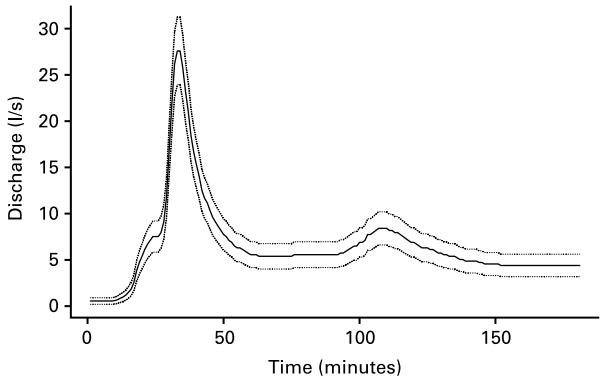

Figure 3 Segment of the hydrograph from Sandsli gauging station. Estimated discharges (solid line) and 95% confidence limits (dotted lines)

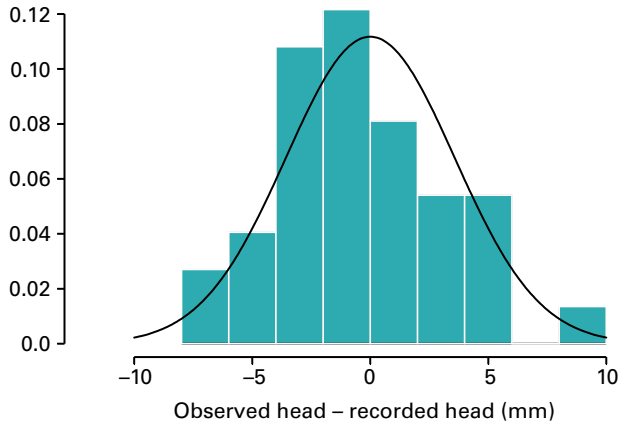

Figure 4 Histogram of the differences between the head values observed at the gauging staff and the recorded heads (control values) at Sandsli gauging station from 2000–2003

$$y \approx x\left(1+\frac{a^{1/b}b\varepsilon}{x^{1/b}}\right) = x + a^{1/b}b\varepsilon x^{1-1/b}. \tag{9}$$

This means that the probability density function (pdf) for the random variable $Y|X$ is given by

$$f_{Y|X}(y|x) = \frac{1}{\sqrt{2\pi}\kappa}\exp\left[-\frac{(y-x)^2}{2\kappa^2}\right], \quad \kappa = b\sigma a^{1/b}x^{1-1/b}. \tag{10}$$

Assuming that the true annual maximum instantaneous discharge has a pdf $f_X(x)$ with parameters σ, the joint pdf of Y and X is, by basic probability theory, given by

$$f_{Y,X}(y,x) = f_{Y|X}(y|x)f_X(x). \tag{11}$$

Furthermore, the marginal pdf for the observed annual maximum instantaneous discharges is given by

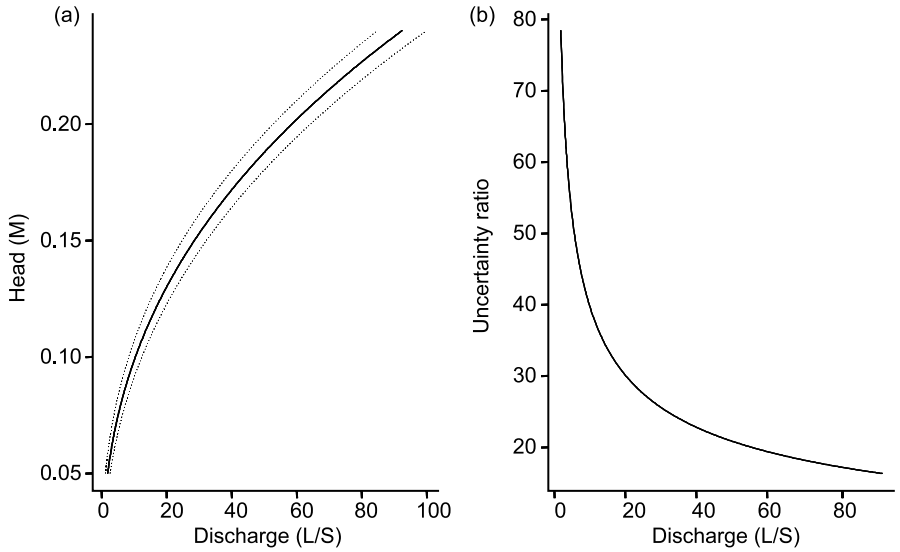

Figure 5 (a) Head–discharge equation for the thin plate v-notch weir at Sandsli gauging station with 95% confidence limits (dotted lines). (b) Uncertainty ratio plot for the estimated discharges at Sandsli gauging station

Table 2 Characteristics of the annual maximum floods at Sandsli

Year	Observed annual maximum head (m)	Estimated annual maximum discharge (l/s)	95% confidence limits (l/s)	Relative uncertainty *R* (%)
1997	0.186	49	(44, 54)	20
1998	0.228	81	(74, 88)	17
1999	0.229	82	(75, 89)	17
2000	0.190	52	(46, 57)	21
2001	0.194	54	(49, 60)	20
2002	n/a	n/a	n/a	n/a
2003	0.237	90	(82, 97)	19

$$f_Y(y) = \int_{-\infty}^{\infty} f_{Y,X}(y,x)\mathrm{d}x. \tag{12}$$

Normally Eq. (12) cannot be evaluated exactly in closed form and must be calculated using numerical integration. Some examples of Eq. (12), assuming that the true instantaneous annual maximum discharge follows a gumbel distribution, are shown in Fig. 6. Figure 6 permits the following observations to be made: 1) the uncertainty in head determination causes no relocation of the mode of the pdf, but alters its shape, seemingly by thickening the tails and increasing the variance and 2) this effect appears to be significant if the coefficient of variation of the true annual maximum instantaneous discharges is very small. These remarks can be shown to be correct observations by introducing the results from Appendix B:

$$E_Y[Y] = E_X[X] \tag{13}$$

$$\mathrm{var}_Y(Y) = \mathrm{var}_X(X) + b^2 a^{2/b} \sigma^2 E_X[X^{2-2/b}] \geq \mathrm{var}_X(X). \tag{14}$$

Equations (13) and (14) illustrate that the coefficient of variation of the error-corrupted annual maximum instantaneous discharges (CV_Y) is greater than the coefficient of variation of the true annual maximum instantaneous discharges (CV_X). Equation (14) is in general difficult to assess analytically. However, note that if $b = 2$ we obtain

$$CV_Y = \sqrt{CV_X^2 + 4\sigma^2 a}. \tag{15}$$

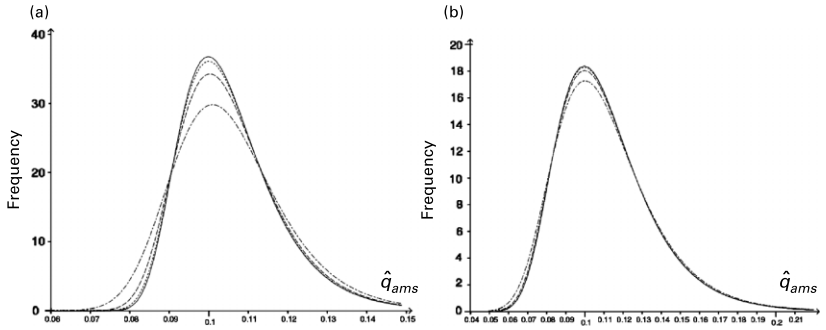

Figure 6 Probability density functions of observed annual maximum instantaneous discharges of which solid lines are $\sigma \approx 0$, dotted lines with lowest mode are $\sigma = 0.0075$, dotted lines with highest mode are $\sigma = 0.002$ and dotted lines with midmost mode are $\sigma = 0.004$. The location and scale parameters of the gumbel distribution of the true annual maximum instantaneous discharges are respectively 0.1 and 0.01 → $CV_Y = 0.1$ (a); and 0.1 and 0.02 → $CV_Y = 0.2$ (b)

Figure 7 gives an overview of the relationship between CV_Y, CV_X and a when $\sigma = 0.0075$ (low accuracy) and $b = 2$. We see that CV_Y is only slightly different from CV_X when CV_X is very small, and that the coefficient of discharge a plays a lesser role. The authors have, by numerical methods, investigated Eq. (14) for other values of b and found that Fig. 7 is representative for most realistic situations. Hence, inaccurate head determination appears to generally cause only a minor potential for bias in estimated flood quantiles for small and urban watersheds, if the observed instantaneous discharge is mistaken for being the true instantaneous discharge. However, subsequent analysis not presented here indicates that the presence of a known σ appears to increase the variability of estimated flood quantiles, since analysis not presented here shows that the likelihood function for the observed annual maximum discharges $L(\theta|(\sigma,a,b)),\sigma \neq 0$, is inflated compared to the likelihood function for the true annual maximum discharges $L(\theta)$. This is analogous to the findings of Kuczera (1992) who investigated the impact of uncorrelated measurement uncertainty in flood frequency inference by simulation.

Conclusions

Although uncertainty in head measurement is well known in operational hydrology, it is commonly neglected in flood analyses for urban and small rural catchments where high time resolution is essential.

This paper shows that instantaneous flood discharges from small urban and rural catchments are significantly corrupted by uncertainty due to inaccurate head measurement, even if the head–discharge equation is free of error. This result should call attention to a significant problem in several research areas which use flood discharge data from small catchments.

A simple error model for head measurement uncertainty is developed and applied to a presumed correct head–discharge equation. The model is based on an unbiased concept and variability equal to hydrometric experiences and figures from manufacturers of hydrometric equipment. Expressions of uncertainty by 95% confidence limits and relative uncertainty of the observed instantaneous discharge and mean discharge are developed. It is shown that uncertainty caused by inaccurate head measurement is negligible for most mean discharges, while it can be substantial for instantaneous flood discharges. The effect of not accounting for head measurement uncertainty is demonstrated by practical modelling using data from a Norwegian urban gauging station. Furthermore, the present study shows how uncertainty in the head causes a negligible potential for bias in estimated flood quantiles and product moments.

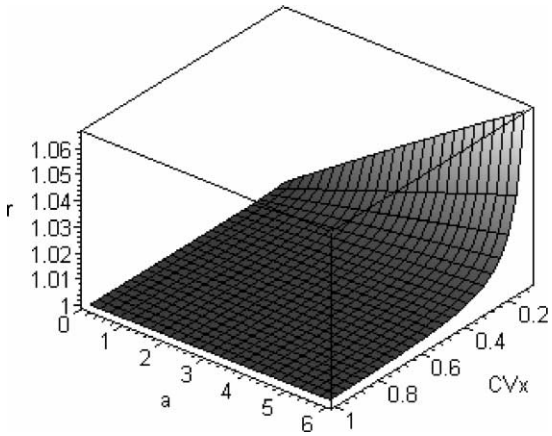

Figure 7 The relationship between $r = CV_X/CV_Y$, CV_Y and a when $b = 2$ and $\sigma = 0.0075$

There are several directions in which future work on the problem should proceed. Similar uncertainty arguments can be extended to calculate the uncertainties arising from inaccurate head measurements in 1) low-flow analysis from larger rural catchments, which involves considering 7-day minimum and deficit volumes at gauging stations with low time resolution, 2) yields of suspended sediment from small catchments which involves use of a second discharge–sediment concentration equation and 3) combination with the uncertainty due to variability in the head–discharge equation.

References

Ackers, P., White, W.R., Perkins, J.A. and Harrison, A.J.M. (1978). *Weirs and Flumes for Flow Measurements*, John Wiley & Sons, Chichester.

Andersen, H.E., Kronvang, B. and Larsen, S.E. (1999). Agricultural practices and diffuse nitrogen pollution in Denmark: empirical leaching and catchment models. *Wat. Sci. Technol.*, **39**(12), 257–264.

Beuselinck, L., Steegen, A., Govers, G., Nachtergaele, J., Takken, I. and Poesen, J. (2000). Characteristics of sediment deposits formed by intense rainfall events in small catchments in the Belgian Loam Belt. *Geomorphology*, **32**, 69–82.

Blake, W.H., Walsh, R.P.D., Barnsley, M.J., Palmer, G., Dyrynda, P. and James, J.G. (2003). Heavy metal concentrations during storm events in a rehabilitated industrialized catchment. *Hydrol. Proc.*, **17**, 1923–1939.

Cerdan, O., Le Bissonnais, Y., Couturier, A. and Saby, N. (2002). Modelling interrill erosion in small cultivated catchments. *Hydrol. Proc.*, **16**, 3215–3226.

Clarke, R.T. (1999). Uncertainty in the estimation of mean annual flood due to rating curve indefinition. *J. Hydrol.*, **222**, 185–190.

Fisher, R.A. and Tippett, L.H.C. (1929). Limiting forms of the frequency distribution of the largest or smallest member of a sample. *Proc. Cambridge Phil. Soc.*, **24**, 180–190.

Herschy, R.W. (1999a). Flow measurements. In R.W. Herschy (Ed.), *Hydrometry: Principles and Practices* (2nd edn.), John Wiley & Sons, Chichester, 9–84.

Herschy, R.W. (1999b). Uncertainties in hydrometric measurements. In R.W. Herschy (Ed.), *Hydrometry: Principles and Practices* (2nd edn.), John Wiley & Sons, Chichester, 355–371.

Keeland, B.D., Dowd, J.F. and Hardgree, W.S. (1997). Use of inexpensive pressure transducers for measuring water levels in wells. *Wetlands Ecol. Mngmnt.*, **5**, 121–129.

Kuczera, G. (1992). Uncorrelated measurement error in flood frequency inference. *Wat. Res. Res.*, **28**(1), 183–188.

La Marche, J.L. and Lettenmaier, D.P. (2000). Effects on forest roads on flood flows in the Deschutes River, Washington. *Earth Surf. Processes Landforms*, **26**(2), 115–134.

Marsalek, J., Barnwell, T.O., Geiger, W.F., Grottker, M., Huber, W.C., Saul, A.J., Schilling, W. and Torno, H.C. (1993). Urban drainage systems: Design and operation. *Wat. Sci. Technol.*, **27**(12), 31–70.

Novotny, V., Clark, D., Griffin, R.J. and Booth, D. (2001). Risk based urban watershed managements under conflicting objectives. *Wat. Sci. Technol.*, **43**(5), 69–78.

Potter, K.W. and Walker, J.F. (1981). A model of discontinuous measurement error and its effect on the probability distribution of flood discharge measurements. *Wat. Res. Res.*, **17**(5), 1506–1509.

Rosso, R. (1985). A linear approach to the influence of discharge measurement error on flood estimates. *Hydrol. Sci.*, **30**(1), 137–149.

World Meteorological Organization (1994). *Guide to Hydrological Practices*, 2nd edn. WMO No.168, Geneva.

Appendix A

The relationship between the observed head $\hat{w}$ and the true head w is given by

$$w = \hat{w} + \sigma\varepsilon, \quad \varepsilon \sim N(0,1). \tag{A1}$$

Thus, the true flood discharge becomes

$$q = aw^b \tag{A2}$$

and the observed flood discharge becomes

$$\hat{q} = a\hat{w}^b = a(\hat{w} + \sigma\varepsilon)^b. \tag{A3}$$

Furthermore, we define

$$\Delta \equiv \hat{q} - q = a(\hat{w} + \sigma\varepsilon)^b - aw^b. \tag{A4}$$

Equations (A1)–(A4) thus give

$$\begin{aligned} F_\Delta(d) &\equiv P(\Delta \le d) = P\{a(w + \sigma\varepsilon)^b - aw^b \le d\} \\ &= P\left\{\varepsilon \le \frac{(d/a + w^b)^{1/b} - w}{\sigma}\right\} = \Phi\left\{\frac{(d/a + w^b)^{1/b} - w}{\sigma}\right\} \end{aligned} \tag{A5}$$

where $\Phi(\cdot)$ is the cumulative distribution of the standard normal distribution. Hence, we have obtained the exact cumulative distribution of Φ. Furthermore, Eq. (A5) implies

$$f_\Delta(d) = F'_\Delta(d) = \frac{(d + aw^b)^{1/b-1}}{\sqrt{2\pi}a^{1/b}b\sigma}\exp\left[-\left\{\frac{(d/a + w^b)^{1/b} - w}{\sqrt{2}\sigma a^{1/b}}\right\}^2\right]. \tag{A6}$$

For $d \ll q \Leftrightarrow d \ll aw^b$ we can perform the approximations

$$\begin{aligned} f_\Delta(d) &\approx \frac{1}{\sqrt{2\pi}ab\sigma w^{b-1}}\exp\left[-\left\{\frac{a^{1/b}w\left(1 + \frac{d}{aw^b}\right)^{1/b} - a^{1/b}w}{\sqrt{2}\sigma a^{1/b}}\right\}^2\right] \\ &\approx \frac{1}{\sqrt{2\pi}ab\sigma w^{b-1}}\exp\left[-\left\{\frac{\frac{d}{abw^b}}{\sqrt{2}\sigma a^{1/b}}\right\}^2\right] \end{aligned} \tag{A7}$$

and obtain the approximation

$$\Delta \sim N\{0, (\sigma abw^{b-1})^2\} = N\{0, (\sigma a^{1/b}bq^{1-1/b})^2\}. \tag{A8}$$

This result can also be obtained from a Taylor expansion of Eq. (A4). Moreover, such an expansion enables us to obtain the higher-order expressions for $E[\Delta]$ and $\mathrm{var}(\Delta)$. First, we need the following result:

$$\begin{aligned} \Delta = a(w + \sigma\varepsilon)^b - aw^b &= aw^b\left\{\left(1 + \frac{\sigma\varepsilon}{w}\right)^b - 1\right\} \approx q\left\{\frac{b\sigma\varepsilon}{w} + \frac{b(b-1)\sigma^2\varepsilon^2}{2w^2}\right\} \\ &= bq^{1-1/b}a^{1/b}\sigma\varepsilon + \frac{1}{2}b(b-1)q^{1-2/b}a^{2/b}\sigma^2\varepsilon^2 \end{aligned} \tag{A9}$$

Thus, we obtain the second-order approximations

$$E[\Delta] = \frac{1}{2}b(b-1)q^{1-2/b}a^{2/b}\sigma^2 = \text{bias} \tag{A10}$$

and

$$\mathrm{var}(\Delta) = b^2q^{2-2/b}a^{2/b}\sigma^2 + \frac{1}{2}b^2(b-1)^2q^{2-4/b}a^{4/b}\sigma^4 \tag{A11}$$

since $\mathrm{cov}(\varepsilon,\varepsilon^2) = 0$.

Considering the squared error:

$$\begin{aligned} \text{squared error} &= \text{variance} + \text{bias}^2 \\ &= b^2q^{2-2/b}a^{2/b}\sigma^2 + \frac{3}{4}b^2(1-b)^2q^{2-4/b}a^{4/b}\sigma^4 \end{aligned} \tag{A12}$$

we see that the second-order terms in both the bias and the variance contribute little to the squared error. Thus, these terms can be ignored and we can conclude that Eq. (A8) is a good approximation.

Appendix B

The results of Appendix A can be used to find the expectation and variance of the marginal distribution of the observed discharges. First, we will consider the second-order approximation. Simplifying the notation by denoting the observed flood discharges Y and the true flood discharges X, we obtain

$$E_Y[Y] = E_X\{E_{Y|X}[X|Y]\} = E_X[X] + \frac{1}{2}b(b-1)a^{2/b}\sigma^2 E_X[X^{1-2/b}] \tag{B1}$$

$$\begin{aligned} \mathrm{var}_Y(Y) &= \mathrm{var}_X\{E_{Y|X}[Y|X]\} + E_X\{\mathrm{var}_{Y|X}(Y|X)\} \\ &= \mathrm{var}_X\left\{X + \frac{1}{2}b(b-1)a^{2/b}\sigma^2 X^{1-2/b}\right\} + b^2 a^{2/b}\sigma^2 E[X^{2-2/b}] \\ &\quad + \frac{1}{2}b^2(b-1)^2 a^{4/b}\sigma^4 E[X^{2-4/b}] \end{aligned} \tag{B2}$$

These expressions are not very tractable, and make it difficult to obtain analytical results in any subsequent analysis. By changing to a first-order approximation we obtain

$$E_Y[Y] = E_X[X] \tag{B3}$$

$$\mathrm{var}_Y(Y) = \mathrm{var}_X(X) + b^2 a^{2/b}\sigma^2 E_X[X^{2-2/b}] \tag{B4}$$

which are easier and more practical expressions. Furthermore, for $1.5 \leq b \leq 2.5$, which is typical for most weirs and flumes (Herschy 1999b), and $0.0020 \leq \sigma \leq 0.0075$., it is evident that the second-order terms are negligible.